Published in final edited form as:
J Magn Reson Imaging. 2012 November ; 36(5): 1234–1240. doi:10.1002/jmri.23694.

Effects of MRI scan acceleration on brain volume measurement consistency

Gunnar Krueger, PhD[1], **Cristina Granziera, MD, PhD**[2], **Pr. Clifford R. Jack Jr., MD**[3], **Pr. Jeffrey L. Gunter, PhD**[3], **Arne Littmann, PhD**[4], **Bénédicte Mortamet, PhD**[1], **Stephan Kannengiesser, PhD**[4], **Pr. Alma Gregory Sorensen, MD**[5], **Chadwick P. Ward**[3], **Denise A. Reyes**[3], **Paula J. Britson**[3], **Hubertus Fischer, PhD**[4], and **Pr. Matt A. Bernstein, PhD.**[3]

[1]Siemens Schweiz AG, Healthcare Sector IM&WS, Renens, Switzerland [2]Neurology Department, CHUV, Lausanne, Switzerland [3]Mayo Clinic and Foundation, Rochester, Minnesota, United States [4]Siemens AG, Healthcare Sector, Erlangen, Germany [5]Siemens Medical Solutions, Healthcare Sector, Malvern, PA, United States

Abstract

Purpose—To evaluate the effects of recent advances in MRI RF coil and parallel imaging technology on brain volume measurement consistency.

Materials and Methods—103 whole-brain MRI volumes were acquired at a clinical 3T MRI, equipped with a 12- and 32-channel head coil, using the T1-weighted protocol as employed in the Alzheimer's Disease Neuroimaging Initiative study with parallel imaging accelerations ranging from 1 to 5. An experienced reader performed qualitative ratings of the images. For quantitative analysis, differences in composite width (CW, a measure of image similarity) and boundary shift integral (BSI, a measure of whole-brain atrophy) were calculated.

Results—Intra- and inter-session comparisons of CW and BSI measures from scans with equal acceleration demonstrated excellent scan-rescan accuracy, even at the highest acceleration applied. Pairs-of-scans acquired with different accelerations exhibited poor scan-rescan consistency only when differences in the acceleration factor were maximized. A change in the coil hardware between compared scans was found to bias the BSI measure.

Conclusion—The most important findings are that the accelerated acquisitions appear to be compatible with the assessment of high-quality quantitative information and that for highest scan-rescan accuracy in serial scans the acquisition protocol should be kept as consistent as possible over time.

Keywords

Magnetic resonance imaging (MRI); brain; measurement consistency

INTRODUCTION

Recent advances in magnetic resonance imaging (MRI) have provided improved signal-to-noise ratios (SNR) through higher magnetic fields and dedicated coil arrays (1,2). Modern commercial 3 Tesla (T) scanners equipped with coil arrays may provide substantial SNR gains compared to 1.5T scanners of a decade ago. The higher SNR is used to improve

Address for correspondence: Dr Gunnar Krueger, Siemens Schweiz AG, Healthcare Sector IM&WS, Avenue des Baumettes 5, 1020 Renens/Lausanne, Switzerland, Tel: +41 79 219 7845, Fax: +41 585 542 879, gunnar.krueger@siemens.com.

sensitivity, spatial resolution and to apply parallel imaging methods for accelerated clinical protocols (3–8).

Structural imaging is one of the MR applications that may greatly benefit from accelerated acquisitions. This is, as the method is prone to motion artifacts, in particular when examining elderly and cognitively impaired patients with reduced tolerance for scans of several minutes duration. Despite the motion sensitivity, structural MRI is a recognized technique to assess disease progression in dementia patients, often by measuring rates of brain atrophy in serial scans. Using the boundary shift integral (BSI) approach (9), whole-brain atrophy in Alzheimers's disease (AD) patients and in healthy controls has ranges between 1% – 2.78% and 0.2% – 0.54%, respectively (9–16).

In this work, we explore the potential of the latest clinical 3T platforms to substantially lower scan times of brain imaging protocols used for morphometric analysis. We employed the composite width (CW, (13)) – a measure of serial scan consistency – the whole brain and ventricular BSI metrics as sensitive quantitative methods to investigate whether and how quantitative results and diagnostic performance may be affected by the protocol changes.

MATERIALS AND METHODS

Subjects

The institutional review board approved this HIPAA-compliant study. Before the examinations, written informed consent was obtained from all four healthy subjects (26 ± 6 years, 2 male and 2 female). None had history of previous neurological illness or alcoholism.

MR Acquisition

All measurements were performed on a clinical 3T Siemens system (MAGNETOM Trio, A Tim System, syngo MR B13 software) equipped with a product version of a 32-channel receive-only head coil (1).

In each session, 12 MPRAGE volumes were acquired using the 32-channel coil and the T1-weighted ADNI protocol (17–19) at 6 different acceleration factors (AF): without parallel imaging (AF=1, 9:15 min), with AF=2 (5:29 min), AF=3 (3:56 min), AF=4 (3:26 min), AF=5 (2:54 min) and AF=5+ ("5+" stands for AF=5 with 10% slice oversampling, 2:54 min). The sequence of accelerations was randomized and acquired twice within one session. The 3T ADNI protocol provides a high-resolution 3D volume with 1.0×1.0×1.2 mm voxel size and excellent contrast (TR/TI/TE = 2300/900/6.9 ms) among brain tissues gray matter, white matter and cerebrospinal fluid (17–20).

The acquisition of the 12 MPRAGE volumes was repeated with all subjects within 8 weeks (4.5 ± weeks). In the rescan session, 2 additional volumes were acquired (first subject one volume only) with the standard non-accelerated ADNI MPRAGE protocol using the 12-channel product head coil, leading to a total acquisition of 14 volumes in the rescan session. Summarizing both scan and rescan sessions, in total 26 brain volumes (25 volumes for one subject) were acquired per subject providing a total of 103 volumes that entered the subsequent analysis.

Image reconstruction of accelerated data was performed using the product software implementation of the generalized autocalibrating partially parallel acquisition (GRAPPA) (7). For assessment of signal inhomogeneities introduced in multi-channel receive coil arrays, SNR maps were calculated from two gradient echo scans by pixel-wise division of raw signal data and noise reference scans as described previously (1).

Data Processing and Analysis

Image sets were analyzed both qualitatively and quantitatively. Qualitatively, a trained individual (same person who performed >2000 image quality ratings within the ADNI study) graded all scans for artifacts and overall image quality. A blinded score table was created by visually rating each scan against all other scans within a session: a score of 2 was assigned if a scan was of higher image quality, a score of 1 for equal image quality and 0 for lower image quality than a compared scan. The blinded comparison score represents the sum of scores for each imaging volume, e.g., in the rescan session with 14 scans, a blinded comparison score of 26 would refer to the scan of superior image quality.

All data were run through the ADNI pre-processing pipeline, which includes 3D gradient distortion correction and the non-parametric non-uniform intensity normalization (N3) (17). Corresponding 3D image sets were co-registered for BSI calculation using 9 degree of freedom. The B1-receive field correction was performed using the Siemens-specific “pre-scan normalize” technique (21,22).

For quantitative analysis, the automated boundary shift integral (BSI, (9,11)) and composite width (CW, (13)) analysis was performed.

BSI measures brain volume changes between spatially co-registered volumes through the shift in the brain-CSF interfaces (whole-brain and ventricles) (9). For this purpose, one scan of the serially acquired pair of scans in a subject is labeled the base for calculation of volume changes over time with the matched volume. BSI has been often used to monitor atrophy in AD disease evolution (9–16,23,24), and in therapeutic intervention studies (12). Note that the ventricle BSI is a presentation of the ventricular volume changes between scans. The used algorithm was adapted from Freeborough and Fox (9) and has been adapted with an intensity normalization similar to the recent work of Leung et al (25) for improved insensitivity to acquisition inconsistencies between pairs-of-scans. Brain extraction was done by a single operator using a semi-automated method.

The CW metric represents a sensitive measure to investigate similarity of contrast in serial scans within the same subject and to draw conclusions about within-subject inter-scan compatibility (13). To measure CW difference, histograms of the CSF and white matter (WM) intensity distributions are calculated. Means and widths are determined by fitting Gaussian distributions to the observed spectra. After linear remapping and intensity normalization, the widths of WM and CSF peak distributions of serial scans are compared (13). Based on experience with this metric in research studies at Mayo Clinic Rochester, we considered a more stringent CW score than used in the original publication (13) of < 3% to represent good inter-scan compatibility.

Because of rescan intervals ≤8 weeks, any difference in the BSI and CW measurements is considered as an error due to experimental variations in the MR acquisition (26). Data from inter- and intra-session analysis were combined into one analysis as described below. However, to also assess the differences between intra- and inter-session reliabilities, we also computed the ratios between the inter- and intra-session analyses. More specifically, we calculated the average ratio from the different analyses (e.g. average from 6 AFs for CW at constant AF). The ratio has the following meanings: a value of one indicates identical behavior for the two cases; a ratio greater than one means inter-session reliability is lower than the intra-session and vice versa for a ratio lower than one.

To assess the relevance of experimental variations, the following questions were addressed according to Table 1:

1. Does acceleration of image acquisition influence BSI (whole-brain and ventricle) and CW measures in serial MRIs of the same subject if scan pairs are acquired with equal acceleration (e.g. compare AF=2 volumes from scan and rescan session)?
2. Does pairing of non-accelerated data to scans with increasing acceleration factor influence apparent whole-brain BSI and CW measures?
3. Does comparison of non-accelerated data (12-channel coil) to scans with increasing acceleration factor (32-channel coil) influence apparent BSI (whole-brain and ventricular) and CW measures?

RESULTS

Figures 1A–E show T1-weighted images from one subject at different acceleration factors obtained with the 32-channel coil. Figure 1F shows a corresponding image acquired with the 12-channel head matrix coil. Figure 2 demonstrates an in-vivo SNR map obtained with the 32-channel coil.

All scans were rated by the experienced interpreter to be of outstanding or excellent image quality. Only 5 out of 103 acquired volumes demonstrated mild ghosting artifacts, presumably originating from slight subject motion. Though noise degradation visibly increases with AF, even the 5-fold accelerated images were considered qualitatively as acceptable and clinically useful. Due to the coil design (1), the SNR penalty at high acceleration factors is primarily evident in the center of the brain (compare Figure 1E and Figure 2).

The correlation between qualitative quality ratings (blinded to acceleration factor) and the actual acceleration factor used was high (r=0.96). Images obtained with the 12-channel matrix coil were found to have an average blinded comparison score of 18. Thus, quality of the 12-channel coil images is judged by this blinded comparison to appear between the images obtained with AF=2 (score of 21) and AF=3 (score of 15) with the 32-channel coil (recall the maximum score is 26).

For quantitative analysis, different types of comparisons were performed:

1. Intra- and inter-session comparisons with constant AF, all acquired with the 32-channel coil (left box-chart in Figure 3,4,5):

   The composite width of scan pairs with equal (constant) AF demonstrate excellent scan-rescan consistency at all accelerations with a maximum peak deviation in individual data of 1.52% (CW <3% represents good inter-scan stability). Similarly, whole-brain BSI values from pairs of scans with equal acceleration are fairly homogeneous and close to the expected value of zero % with a maximum peak deviation of 1.1% even at the highest acceleration applied (AF=5). The ventricle BSI shows a similar homogeneous behaviour close to 0 but with larger standard deviations. The averaged ratios between the inter- and intra-session analyses were 1.5 +/− 0.4 (CW), −0.6 +/− 0.3 (BSI) and −1.6 +/− 4.0 (ventricle BSI – in this case excluding 5+ since the denominator was zero), respectively.

   Therefore, the data suggest that greater AF will not influence the test-retest precision when other protocol parameters do not differ between scans.

2. Inter-session comparison between the base scan without acceleration and matched scans with increasing AF, all acquired with the 32-channel coil (center box-chart in Figure 3–5):

Comparing data obtained without acceleration and all AF combinations (AF 1–5+) demonstrates that dissimilarity in CW is substantially increasing at AF 5 and 5+ (>3%), while AF<5 shows acceptable mean CW changes below 2.3% with a maximum peak deviation of 2.7%. Similarly, whole-brain BSI differs only substantially from 0 at AF 5 and 5+. The ventricle BSI appears homogeneous at larger means and standard deviations. It may be noticed that the whole-brain BSI data appear with a slight negative downward bias (with the exception of AF 5+), indicating that repositioning or differences in the shim between the sessions may introduce subtle variances in the results.

These data suggest that subtracting scans with increasing acceleration factor will not influence apparent volume difference up to AF 4 (Hp2), but will at greater AF values.

3. Comparing 32-channel vs. 12-channel data (right box-charts in Figure 3–5):

   The CW method exhibits good reproducibility when comparing 3D MPRAGE volumes obtained with the 12-channel coil without acceleration and volumes acquired with the 32-channel coil for AF<5 (highest similarity at AF 2). For AF 5 and 5+, CW changes exceed the 3% limit.

   Noteworthy, a systematic shift of ~0.5% is observed in whole-brain BSI, which could arise from differences in repositioning and shims after the coil change (27). Similar qualitative behavior is evident in the ventricle BSI. In addition, whole-brain BSI is shifted by about 1 standard deviation for AF=5.

   The ratios between the inter- and intra-session analyses were 1.2 +/− 0.3 (CW), −1.3 +/− 1.2 (BSI) and −2.9 +/− 2.0 (ventricle BSI), respectively.

DISCUSSION

The results from the qualitative and quantitative analysis suggest that: a) all accelerated data – even with 5-fold acceleration – may be diagnostically valuable as radiologists typically can “read through” artifacts and inhomogeneous noise distributions, b) provided consistent hardware and protocol settings are used, all images including those with the highest acceleration demonstrate excellent scan-rescan consistency and indicate clinical usefulness for automated evaluation procedures of serial scans, c) when comparing data of increasing acceleration factors with the non-accelerated data (32-channel coil), CW and whole brain BSI (ventricle BSI show qualitative similar behavior) demonstrate good inter-scan reproducibility for AF<5, rendering these data as useful for quantitative analysis, and d) changes in the coil hardware between scan pairs in serial scans have to be considered with care since a bias in quantitative measures (BSI) could hamper the data interpretation.

We emphasize that in the longitudinal study of any single subject, highest scan-rescan reproducibility is of particular importance. As an example, a change from the 12- to the 32-channel coil caused a shift in the whole brain BSI of ~0.5%. This systematic bias is unacceptable in quantitative measures derived from serial scans as it corresponds to the annual atrophy rate in controls (9–16). Similarly, unacceptable CW values were observed, when AF changes were maximized (5x vs. non-accelerated). Thus, any hardware and protocol change throughout the course of a longitudinal study may lead to subtle but measurable artifactual changes in the inter-scan reproducibility and should be avoided unless there is specific crossover data to support the change.

Interestingly, the observation that CW and BSI differences are unchanged and their variances did not change significantly at the sensitivity level of the study for scan pairs with constant AF suggests that SNR reductions even with AF=5 do not impair the quality of the

type of quantitative brain volume analysis performed here. The shorter scan time through accelerated acquisition should improve patient acceptance and we expect a reduction of motion artifacts, in particular when examining elderly and cognitively impaired patients. Similarly, the ratio of inter- and intra-session reliabilities is close to one but in most cases greater, indicating that inter-session and intra-session are very comparable, though effects from repositioning and shim changes between session may slightly reduce reliabilities.

It has to be pointed out that the current study design with the involvement of healthy young subjects, particular scanning hardware and dedicated processing strategies has limits and does not allow generalizing all the conclusions. More detailed, this investigation aims at gaining a better understanding of the potential of state-of-the-art hardware to improve anatomical brain imaging protocols. We based our analysis on metrics (CW, whole brain and ventricle BSI) that are sensitized to measure within-subject, inter-scan compatibility and to monitor brain volume changes over time, a methodology that has been demonstrated to provide sensitive markers of structural brain changes in serial scans (9–16,20,23,24). Even though we may expect that the findings would be reproducible in older and diseased patient populations, a number of influencing factors will require more careful investigations. As described recently (1), the 32-channel coil provides the highest SNR in the proximity of the individual coil elements (Figure 2), which makes this approach particularly efficient when cortical measurements are the subject of investigation. Though the whole-brain BSI measure is sensitive to acquisition non-idealities (28), it may particular benefit from the SNR profile of the coil which favors cortical structural elements. Measures other than CW and BSI, such as whole-brain voxel-wise analysis (29–32) or analysis of the hippocampal volume located closer to the center of the coil may exhibit different dependencies on the coil performance, e.g. a dedicated hippocampus analysis may suffer from SNR limitations at the higher accelerations. It should be noted, however, that the dedicated coil hardware is capable to improve SNR considerable even in brain regions located in the coil center when compared to previous generation hardware. Thus, at least the SNR penalty will be compensated with the use of such dedicated coils when using low acceleration factors. This is also supported by the results from the ventricle BSI analysis, which demonstrated homogeneous means and variances at constant AFs (Figure 5). The higher means and standard deviation observed in the ventricle BSI data is rather constant across AFs, suggesting that the SNR differences at various AFs do not influence the analysis. Therefore, the higher variance in these data compared to the whole brain BSI may be largely explained by the smaller ventricle structure in the healthy young subjects investigated here, which implies stronger effects from partial volume contaminations.

Furthermore, the algorithms for reconstruction of the accelerated images (here k-space GRAPPA) also have to be taken into account as they may (a) introduce subtle k-space filtering thereby influencing the outcome measures, or (b) amplify artifact patterns arising from subject motion during the acquisition of the reference data or from residual reconstruction limitations in the presence of spatially varying noise figures, i.e. when changing the acceleration factors between pairs-of-scans. In other words, different target applications including those aiming at regional analysis of brain tissues and structures may operate in a particular SNR limited regime or may specifically rely on a homogeneous noise distribution that could render the use of certain or even any acceleration prohibitive without algorithmic adaptations. Moreover, older and demented patients have different MRI characteristics (including larger ventricles) than the young subjects investigated here (33), which may further modulate the findings.

In conclusion, applying parallel imaging technology to a T1-weighted MRI protocol designed to monitor AD disease progression within the ADNI study, allowed a scan time reduction from 9:12 to 2:54 minutes. Resulting images were qualitatively rated to be of

excellent quality. The accelerated acquisitions appeared to be compatible with the assessment of high-quality quantitative information. We conclude, however, that for highest scan-rescan accuracy and maximized power to detect brain changes in clinical investigations and population studies, the imaging protocol and hardware should be kept as consistent as possible over time.

Acknowledgments

Funding: partial funding from NIH AG24904 and AG11378.

The authors thank Karsten Jahns and Daniel Driemel, Siemens Healthcare Sector, Erlangen, Germany, for their support of this investigation. This work was supported by the Centre d'Imagerie BioMédicale (CIBM) of the University of Lausanne (UNIL), the Swiss Federal Institute of Technology Lausanne (EPFL), the University of Geneva (UniGe), the Centre Hospitalier Universitaire Vaudois (CHUV), Hôpitaux Universitaires de Genève (HUG) and the Leenaards and the Jeantet Foundations.

References

1. Wiggins GC, Triantafyllou C, Potthast A, Reykowski A, Nittka M, Wald LL. 32-channel 3 Tesla receive-only phased-array head coil with soccer-ball element geometry. Magn Reson Med. 2006; 56(1):216–223. [PubMed: 16767762]
2. Roemer PB, Edelstein WA, Hayes CE, Souza SP, Mueller OM. The NMR phased array. Magn Reson Med. 1990; 16(2):192–225. [PubMed: 2266841]
3. Bernstein MA, Huston J 3rd, Lin C, Gibbs GF, Felmlee JP. High-resolution intracranial and cervical MRA at 3. 0T: technical considerations and initial experience. Magn Reson Med. 2001; 46(5):955–962. [PubMed: 11675648]
4. Kruger G, Kastrup A, Glover GH. Neuroimaging at 1.5 T and 3. 0 T: comparison of oxygenation-sensitive magnetic resonance imaging. Magn Reson Med. 2001; 45(4):595–604. [PubMed: 11283987]
5. Bammer R, Skare S, Newbould R, et al. Foundations of advanced magnetic resonance imaging. NeuroRx. 2005; 2(2):167–196. [PubMed: 15897944]
6. Pruessmann KP, Weiger M, Scheidegger MB, Boesiger P. SENSE: sensitivity encoding for fast MRI. Magn Reson Med. 1999; 42(5):952–962. [PubMed: 10542355]
7. Griswold MA, Jakob PM, Heidemann RM, et al. Generalized autocalibrating partially parallel acquisitions (GRAPPA). Magn Reson Med. 2002; 47(6):1202–1210. [PubMed: 12111967]
8. Sodickson DK, Manning WJ. Simultaneous acquisition of spatial harmonics (SMASH): fast imaging with radiofrequency coil arrays. Magn Reson Med. 1997; 38(4):591–603. [PubMed: 9324327]
9. Freeborough PA, Fox NC. The boundary shift integral: an accurate and robust measure of cerebral volume changes from registered repeat MRI. IEEE Trans Med Imaging. 1997; 16(5):623–629. [PubMed: 9368118]
10. Bradley KM, Bydder GM, Budge MM, et al. Serial brain MRI at 3–6 month intervals as a surrogate marker for Alzheimer's disease. Br J Radiol. 2002; 75(894):506–513. [PubMed: 12124237]
11. Ezekiel F, Chao L, Kornak J, et al. Comparisons between global and focal brain atrophy rates in normal aging and Alzheimer disease: Boundary Shift Integral versus tracing of the entorhinal cortex and hippocampus. Alzheimer Dis Assoc Disord. 2004; 18(4):196–201. [PubMed: 15592130]
12. Fox NC, Black RS, Gilman S, et al. Effects of Abeta immunization (AN1792) on MRI measures of cerebral volume in Alzheimer disease. Neurology. 2005; 64(9):1563–1572. [PubMed: 15883317]
13. Gunter JL, Shiung MM, Manduca A, Jack CR Jr. Methodological considerations for measuring rates of brain atrophy. J Magn Reson Imaging. 2003; 18(1):16–24. [PubMed: 12815635]
14. Jack CR Jr, Shiung MM, Gunter JL, et al. Comparison of different MRI brain atrophy rate measures with clinical disease progression in AD. Neurology. 2004; 62(4):591–600. [PubMed: 14981176]

15. O'Brien JT, Paling S, Barber R, et al. Progressive brain atrophy on serial MRI in dementia with Lewy bodies, AD, and vascular dementia. Neurology. 2001; 56(10):1386–1388. [PubMed: 11376193]
16. Wang D, Chalk JB, Rose SE, et al. MR image-based measurement of rates of change in volumes of brain structures. Part II: application to a study of Alzheimer's disease and normal aging. Magn Reson Imaging. 2002; 20(1):41–48. [PubMed: 11973028]
17. Leow AD, Klunder AD, Jack CR Jr, et al. Longitudinal stability of MRI for mapping brain change using tensor-based morphometry. Neuroimage. 2006; 31(2):627–640. [PubMed: 16480900]
18. Jack CR Jr, Bernstein MA, Fox NC, et al. The Alzheimer's disease neuroimaging initiative (ADNI): MRI methods. J Magn Reson Imaging. 2008
19. http://www.loni.ucla.edu/ADNI/Research/Cores/ADNI_Siemens_3T_TrioTimVB13.pdf
20. Jack CR Jr, Bernstein MA, Borowski BJ, et al. Update on the magnetic resonance imaging core of the Alzheimer's disease neuroimaging initiative. Alzheimers Dement. 2010; 6(3):212–220. [PubMed: 20451869]
21. Narayana PA, Brey WW, Kulkarni MV, Sievenpiper CL. Compensation for surface coil sensitivity variation in magnetic resonance imaging. Magn Reson Imaging. 1988; 6(3):271–274. [PubMed: 3398733]
22. Boyes RG, Gunter JL, Frost C, et al. Intensity non-uniformity correction using N3 on 3-T scanners with multichannel phased array coils. Neuroimage. 2008; 39(4):1752–1762. [PubMed: 18063391]
23. Schott JM, Price SL, Frost C, Whitwell JL, Rossor MN, Fox NC. Measuring atrophy in Alzheimer disease: a serial MRI study over 6 and 12 months. Neurology. 2005; 65(1):119–124. [PubMed: 16009896]
24. Whitwell JL, Jack CR Jr. Neuroimaging in dementia. Neurol Clin. 2007; 25(3):843–857. viii. [PubMed: 17659193]
25. Leung KK, Clarkson MJ, Bartlett JW, et al. Robust atrophy rate measurement in Alzheimer's disease using multi-site serial MRI: tissue-specific intensity normalization and parameter selection. Neuroimage. 2010; 50(2):516–523. [PubMed: 20034579]
26. Rohlfing T, Sullivan EV, Pfefferbaum A. Deformation-based brain morphometry to track the course of alcoholism: differences between intra-subject and inter-subject analysis. Psychiatry Res. 2006; 146(2):157–170. [PubMed: 16500088]
27. Littmann A, Guehring J, Buechel C, Stiehl HS. Acquisition-related morphological variability in structural MRI. Acad Radiol. 2006; 13(9):1055–1061. [PubMed: 16935717]
28. Preboske GM, Gunter JL, Ward CP, Jack CR Jr. Common MRI acquisition non-idealities significantly impact the output of the boundary shift integral method of measuring brain atrophy on serial MRI. Neuroimage. 2006; 30(4):1196–1202. [PubMed: 16380273]
29. Vemuri P, Gunter JL, Senjem ML, et al. Alzheimer's disease diagnosis in individual subjects using structural MR images: validation studies. Neuroimage. 2008; 39(3):1186–1197. [PubMed: 18054253]
30. Stonnington CM, Tan G, Kloppel S, et al. Interpreting scan data acquired from multiple scanners: a study with Alzheimer's disease. Neuroimage. 2008; 39(3):1180–1185. [PubMed: 18032068]
31. Kloppel S, Stonnington CM, Barnes J, et al. Accuracy of dementia diagnosis: a direct comparison between radiologists and a computerized method. Brain. 2008; 131(Pt 11):2969–2974. [PubMed: 18835868]
32. Kloppel S, Stonnington CM, Chu C, et al. Automatic classification of MR scans in Alzheimer's disease. Brain. 2008; 131(Pt 3):681–689. [PubMed: 18202106]
33. Salat DH, Greve DN, Pacheco JL, et al. Regional white matter volume differences in nondemented aging and Alzheimer's disease. Neuroimage. 2009; 44(4):1247–1258. [PubMed: 19027860]

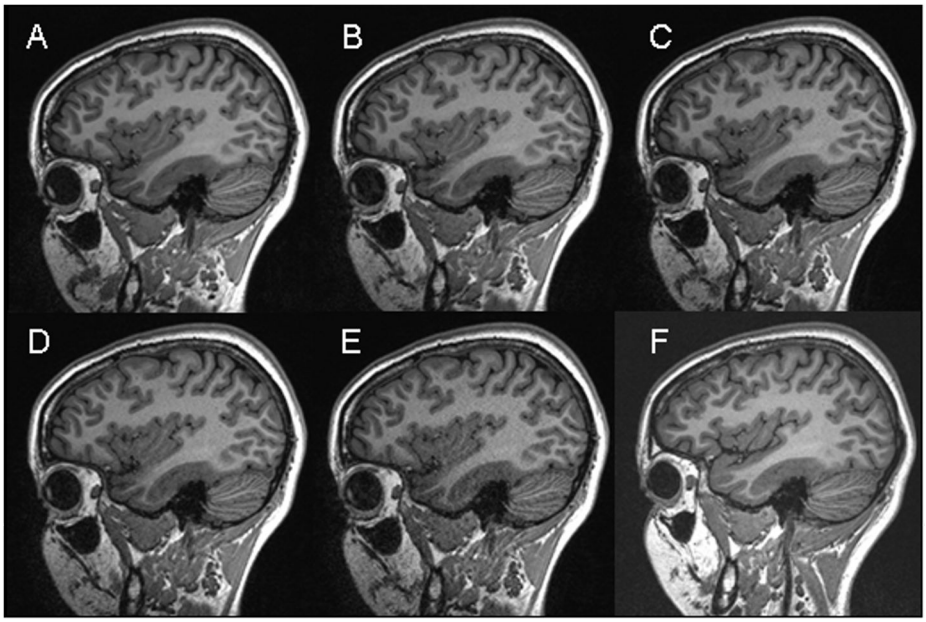

Figure 1.
High-resolution T1-weighted MPRAGE images (TR/TI/TE/flip = 2300/900/6ms/9°, 1.0×1.0×1.2 mm^3, matrix = 240×256) from one subject acquired with the 32-channel head coil without acceleration (A), and with 2-, 3-, 4- and 5-fold acceleration (B–E). A corresponding image acquired at the end of the rescan session using the standard 12-channel head matrix product coil without acceleration is shown in (F).

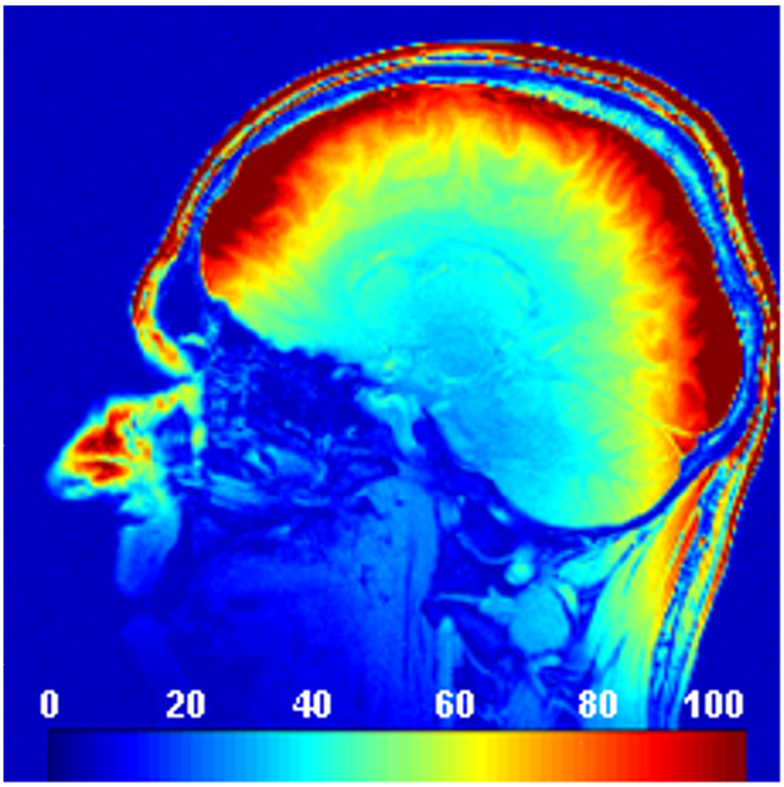

Figure 2.
In-vivo SNR maps were obtained from one subject and computed from two proton density gradient echo scans (TR/TE/flip=200/3.92/30°, slice thickness = 8 mm, matrix = 256×256, FoV = 256 mm, BW=300 Hz/px) using the 32-channel coil. One of the scans was performed without RF transmission to obtain the noise characteristics. SNR values are color coded in a range from 0 to 100 as indicated by the bar in the bottom of the image.

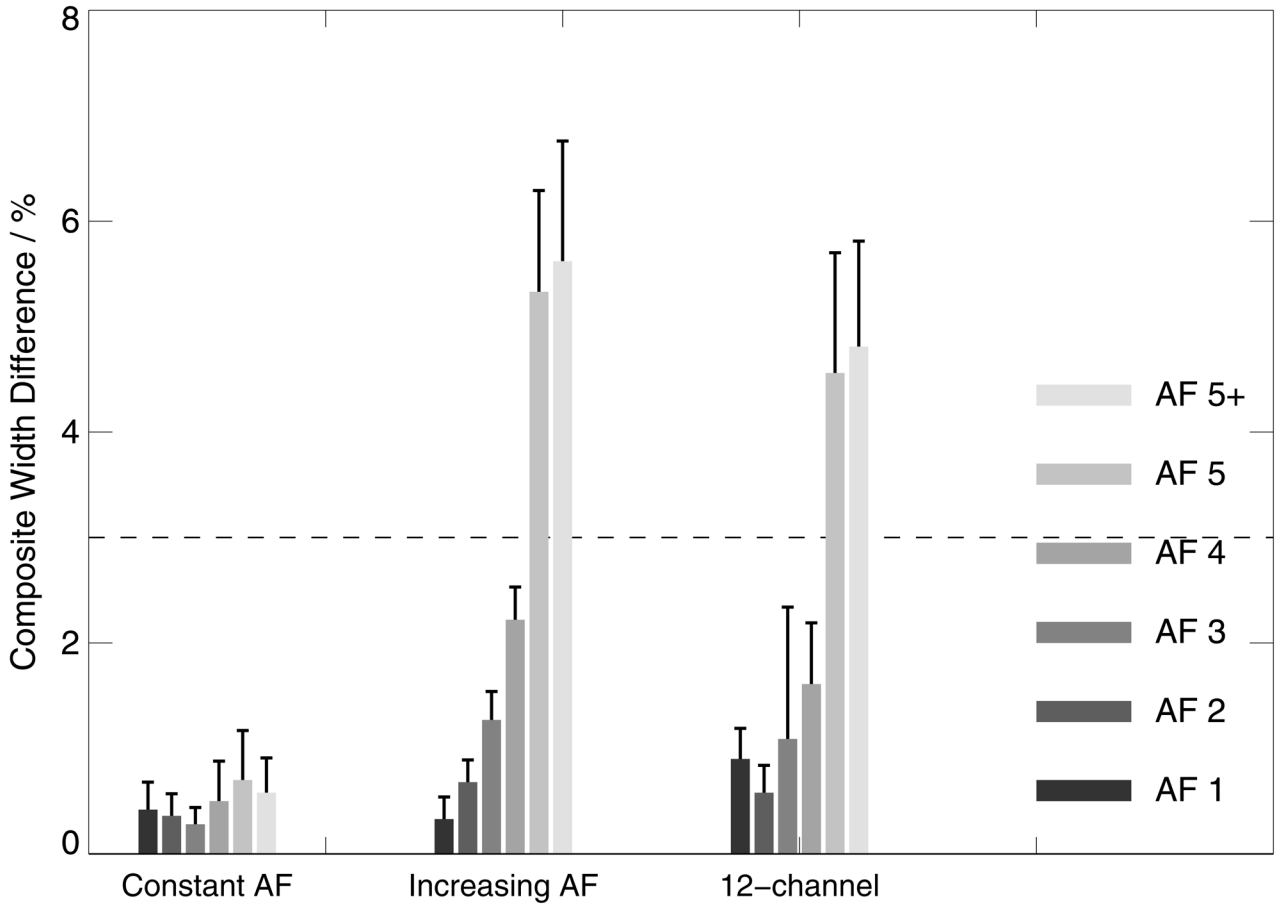

Figure 3.
Composite width differences (boxes indicate mean CW values and error bars standard deviation) for intra- and inter-scan comparisons at constant AF on 32-channel systems (left), with increasing AF on 32-channel systems (center) and comparing the 12-channel base images with 32-channel images at progressively greater AF (right). Excellent scan-rescan accuracy is observed at all accelerations at constant AF and for AF<5 when comparing data with increasing AFs and the 12-channel data. The 3%-line indicates the CW-level which is considered to represent good inter-scan compatibility.

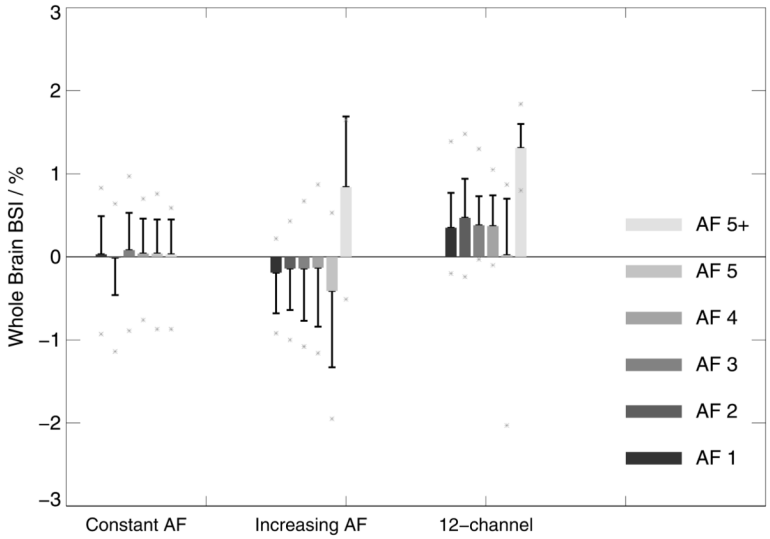

Figure 4.

Whole-brain BSI changes (boxes indicate mean BSI values and error bars standard deviation, asterisk symbols indicate individual peak data) for intra-and inter-scan comparisons at constant AF on 32-channel systems (left), with increasing AF on 32-channel systems (center) and comparing 12-channel base images with 32-channel images with progressively greater AF (right). Excellent scan-rescan accuracy is observed at all accelerations at constant AF. When comparing data with increasing AFs, data exhibits increased levels of BSI changes with progressively increasing variances at higher AFs. In this respect, it also can be observed that the AF=5+ data appear with a different sign, which may reflect subtle but measurable differences in the image contrast when oversampling is used, which slightly affects the magnetization throughout the experiment. Similar patterns are seen when comparing with the 12-channel data. However, a systematic shift of ~0.5% is observed, which could arise from differences in repositioning and shims after the coil change.

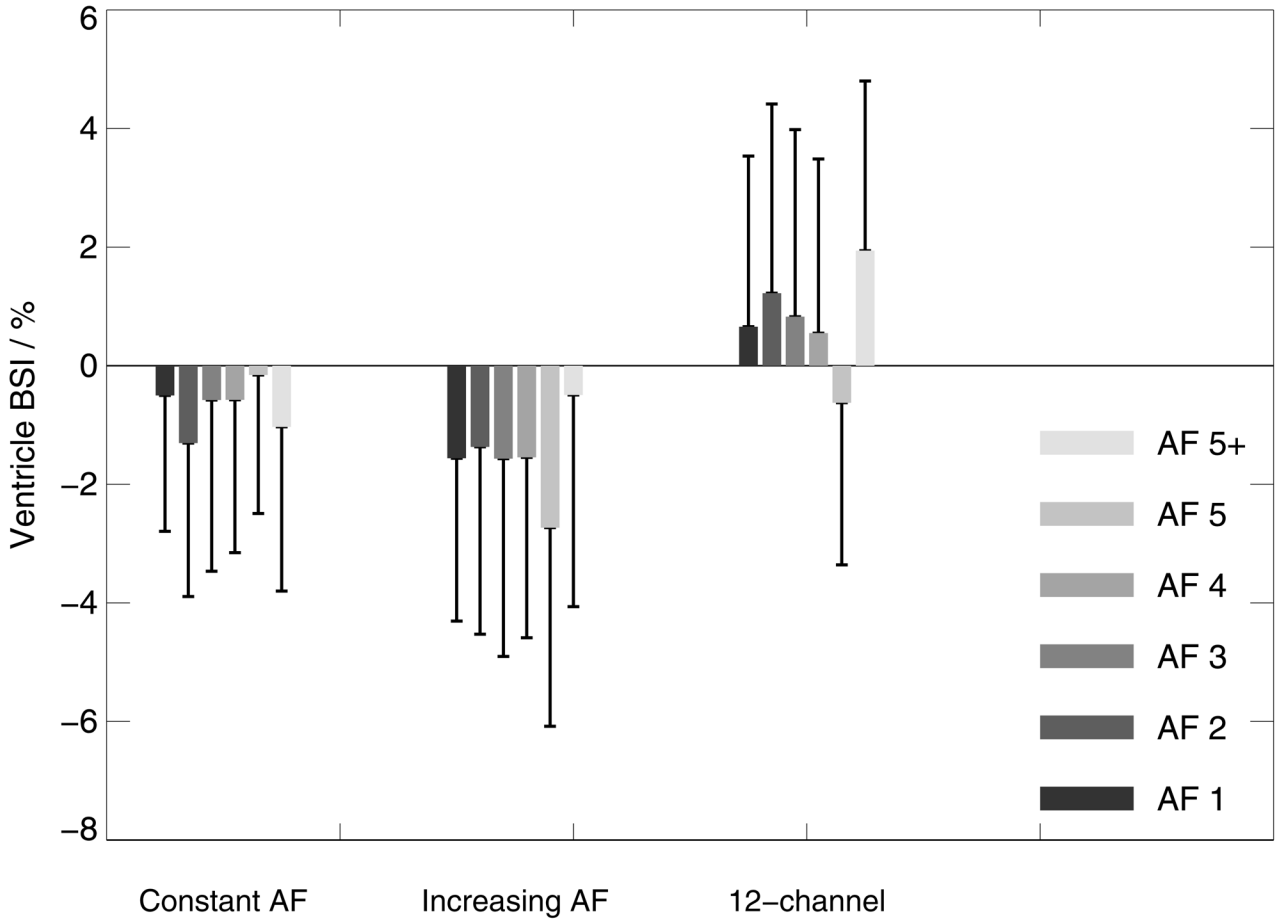

Figure 5.
Ventricle BSI changes (boxes indicate mean ventricle BSI values and error bars standard deviation) for intra- and inter-scan comparisons at constant AF on 32-channel systems (left), with increasing AF on 32-channel systems (center) and comparing 12-channel base images with 32-channel images with progressively greater AF (right).

Table 1

Combinations of MPRAGE pairs-of-scans for computations of BSI and CW

	Constant AF (N=16)	Increasing AF (N=8)	12-channel (N=16)
Intra-session	t1F – t1R t2F – t2R		mpr12 – t2F mpr12 – t2R
Inter-session	t1F – t2F t1R – t2R	t1F (AF=1) – t2A t1F (AF=1) – t2R	mpr12 – t1F mpr12 – t1R

"t1" and "t2" refers to the first and second scan session, respectively, maximum of 8 weeks apart. "F" and "R" refers to first MPRAGE scan and MPRAGE repeat scan within a session. 12-channel scans are labelled "mpr12". Combinations were tested for each of the four subjects and each AF unless indicated.